Joule

CellPress

Article

Oxide layer coating enabling oxysulfide-based photocatalyst sheet to drive Z-scheme water splitting at atmospheric pressure

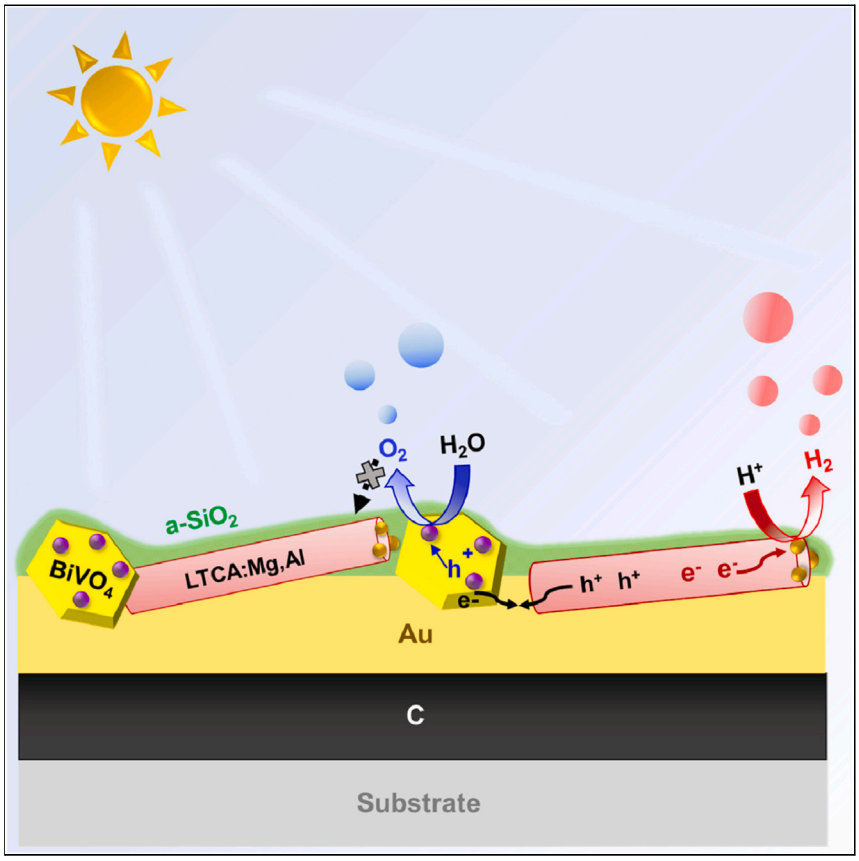

Particulate photocatalyst sheet is one of the approaches to realize solar hydrogen production with high efficiency on a large scale via water splitting. However, the solar-to-hydrogen energy conversion efficiency (STH) of sheets made of narrow band-gap oxysulfide photocatalysts decreases with increasing reaction pressure due to backward reactions. This study addresses this issue through surface modification. An amorphous silica coating can effectively suppress the oxygen reduction reaction (ORR), allowing the sheet to maintain its STH value at elevated pressures and temperatures.

Swarnava Nandy, Takashi Hisatomi, Mamiko Nakabayashi, ..., Naoya Shibata, Tsuyoshi Takata, Kazunari Domen

domen@chemsys.t.u-tokyo.ac.jp

Highlights

Photocatalyst sheets made of $La_5Ti_2Cu_{0.9}Ag_{0.1}O_7S_5$ (LTCA) and $BiVO_4$ split water

Backward reactions on LTCA suppress the STH at elevated pressure

SiO_2 coating allows the photocatalyst sheet to maintain an STH of 0.41% at 90 kPa

Pathways to activate photocatalyst sheets under realistic conditions are identified

Nandy et al., Joule 7, 1–11
July 19, 2023
https://doi.org/10.1016/j.joule.2023.05.018

Please cite this article in press as: Nandy et al., Oxide layer coating enabling oxysulfide-based photocatalyst sheet to drive Z-scheme water splitting at atmospheric pressure, Joule (2023), https://doi.org/10.1016/j.joule.2023.05.018

Joule

CellPress

Article

Oxide layer coating enabling oxysulfide-based photocatalyst sheet to drive Z-scheme water splitting at atmospheric pressure

Swarnava Nandy,[1] Takashi Hisatomi,[1,2] Mamiko Nakabayashi,[3] Huihui Li,[1] Xiaojun Wang,[1] Naoya Shibata,[3] Tsuyoshi Takata,[1] and Kazunari Domen[1,4,5,*]

SUMMARY

A photocatalyst sheet consisting of doped $La_5Ti_2Cu_{0.9}Ag_{0.1}O_7S_5$ as a hydrogen evolution photocatalyst (HEP), $BiVO_4$ as an oxygen evolution photocatalyst (OEP), and Au as a conductor layer exhibits a solar-to-hydrogen energy conversion efficiency (STH) of 0.67% at 4 kPa in Z-scheme overall water splitting (ZOWS). However, the photocatalyst sheet loses its activity at elevated pressure due to backward reactions. Here, we show that this loss of activity can be suppressed by coating the sheet with amorphous SiO_2 layer. In addition, the SiO_2 coating maintained its performance at elevated temperatures, unlike the widely used amorphous TiO_2 coating, and exhibited an STH of 0.41% at 90 kPa and 333 K. The results of the present study demonstrate the ability to functionalize photocatalyst sheets of narrow-band-gap materials prone to backward reactions, allowing their use in outdoor environments, and paves the way for practical solar hydrogen production.

INTRODUCTION

Photocatalytic water splitting using particulate semiconductors has been studied as a means to produce renewable H_2 using sunlight.[1–3] One of the primary challenges in making photocatalytic solar H_2 production economically viable is to develop water splitting systems capable of delivering a solar-to-hydrogen energy conversion efficiency (STH) of 5% or higher. Al-doped $SrTiO_3$ (STO:Al) photocatalysts exhibit an excellent apparent quantum yield (AQY) exceeding 90% in the overall water splitting (OWS) reaction under ultraviolet light.[4] Moreover, a 100-m^2 scale photocatalyst panel reactor operating under ambient conditions was demonstrated using STO:Al.[5] However, STO:Al cannot utilize visible light, which accounts for the majority of solar energy, and its maximum STH value is inevitably insufficient to accomplish the target STH value. In this context, it is vital to utilize visible light (with wavelengths of 400–800 nm). Although some doped oxide and non-oxide semiconductor photocatalysts show OWS activity under visible light, their AQY and STH are several times lower than those for STO:Al in the ultraviolet region, due in part to their inherently lower reactivity stemming from their narrower band gaps.[3,4,6–9]

To compensate for this low reactivity, narrow-band-gap photocatalysts are often used in Z-scheme OWS (ZOWS) systems that utilize two-step excitation of hydrogen and oxygen evolution photocatalysts (HEPs and OEPs, respectively).[10–13] Electron transfer from an OEP to a HEP can occur simply via physical contact, but most often ionic or solid electron mediators are used to facilitate this transfer. Efficient ZOWS was reported for photocatalyst sheets composed of Rh, La co-doped $SrTiO_3$, and

CONTEXT & SCALE

Renewable hydrogen production by sunlight-driven photocatalytic water splitting is studied to address energy and environmental problems. A solar-to-hydrogen energy conversion efficiency (STH) exceeding 5% and inherent scalability beyond the kilometer scale are essential for practical solar hydrogen production. Particulate photocatalyst sheets can potentially meet these requirements. However, the STH of sheets made of narrow band-gap oxysulfide photocatalysts decreases with increasing reaction pressure due to backward reactions. This study addresses this issue through surface modification. We show that an amorphous silica coating is durable in hot water and can effectively suppress the oxygen reduction reaction (ORR), a major backward reaction, allowing the sheet to maintain its STH value at elevated pressures and temperatures, making the resulting sheets suitable for practical outdoor applications. This finding will contribute to the development of practical solar hydrogen production.

Please cite this article in press as: Nandy et al., Oxide layer coating enabling oxysulfide-based photocatalyst sheet to drive Z-scheme water splitting at atmospheric pressure, Joule (2023), https://doi.org/10.1016/j.joule.2023.05.018

Mo-doped $BiVO_4$ (BVO:Mo) as the HEP and OEP, respectively, embedded rigidly onto a conductive layer of gold, carbon, or indium tin oxide to minimize the contact resistance.[14–16] A photocatalyst sheet based on a carbon conductor exhibited an STH of 1.0% at near-ambient pressure. These oxide-based photocatalysts can utilize visible light up to wavelengths of only approximately 500–520 nm. This eventually limits the STH efficiency the sheet can reach.

To utilize visible light with longer wavelengths, photocatalyst sheets composed of narrower band-gap non-oxide HEPs have been studied. Our group has reported that $La_5Ti_2Cu_{0.9}Ag_{0.1}O_7S_5$ (LTCA)[10] and $LaMg_{1/3}Ta_{2/3}O_2N$[17] are applicable as HEPs. These materials absorb visible light with wavelengths of up to 690 and 600 nm, respectively, and have the potential to go beyond the earlier sheet systems, including Rh and La co-doped $SrTiO_3$ as the HEP, owing to the broader visible light response. Of these, LTCA, a solid solution of $La_5Ti_2CuO_7S_5$ (LTC) and $La_5Ti_2AgO_7S_5$ (LTA), is a unique and promising material because its semiconducting and photoelectrochemical properties can be tuned by the composition and the dopants used.[18,19] Doping at the Ti^{4+} sites of LTCA with lower-valent cations (e.g., Ga^{3+}, Mg^{2+}, Al^{3+}, and Sc^{3+}) promotes the performance as a photocathode, realizing a positive photocathodic current onset potential of +0.85 V vs. reversible hydrogen electrode (RHE).[20] These characteristics of LTCA offer advantages for construction of photocatalyst sheets for ZOWS, because the charge transfer mechanism in solid materials is similar for photocatalyst sheets and photoelectrode systems. In contrast, $LaMg_{1/3}Ta_{2/3}O_2N$ is an n-type semiconductor, and its performance as a HEP for photocatalyst sheets was limited. A photocatalyst sheet comprising Ga-doped LTCA (LTCA:Ga), BVO:Mo and Au (denoted as LTCA:Ga/Au/BVO:Mo) modified with Cr_2O_3 shell/Rh core and CoO_x cocatalysts exhibited an STH of 0.4% under reduced pressure.[21] However, the LTCA:Ga/Au/BVO:Mo sheet was less active than a sheet employing Rh and La co-doped $SrTiO_3$ as the HEP. Moreover, it suffered from a strong pressure dependence of ZOWS activity, which decreased to less than half as the background pressure was increased from 2 to 20 kPa due to backward reactions involving water formation from hydrogen and oxygen and the oxygen reduction reaction (ORR). Other groups also study ZOWS systems operable under long-wavelength visible light. For example, Zhao et al. reported an STH value of 1.16% by using a ZOWS system based on doped C_3N_4 photocatalysts containing a Pt cocatalyst without any surface modification.[22] However, the activity of the Z-scheme system at elevated pressure has been rarely examined. This is a critical problem for practical renewable hydrogen production via photocatalytic OWS, in which operation at atmospheric pressure is anticipated.[5,23] This study addresses this issue through surface modification of the photocatalyst sheet. We show that surface modification of a photocatalyst sheet composed of Mg- and Al-co-doped LTCA (LTCA:Mg,Al), Mo-doped BVO (BVO:Mo), and Au as the HEP, OEP, and conductive layer, respectively, modified with Cr_2O_3/Rh and CoO_x as reduction and oxidation cocatalysts, respectively, with an amorphous SiO_2 layer effectively suppresses the ORR while preserving the HEP and OEP activity, allowing the photocatalyst sheet to maintain an STH of 0.41% at near-ambient pressure, whereas it drops to 0.01% without the modification.

RESULTS AND DISCUSSION

Physical properties of synthesized photocatalysts

As shown in Figure S2A, the X-ray diffraction (XRD) patterns for LTCA:Mg,Al and LTCA:Ga exhibit characteristic peaks attributable to the LTCA phase.[10,21] Figure S2B shows UV-vis diffuse-reflectance spectra (DRS), which indicate an absorption onset

[1]Research Initiative for Supra-Materials, Interdisciplinary Cluster for Cutting Edge Research, Shinshu University, 4-17-1 Wakasato, Nagano 380-8553, Japan

[2]PRESTO, JST, 4-17-1 Wakasato, Nagano-shi, Nagano 380-8553, Japan

[3]Institute of Engineering Innovation, School of Engineering, The University of Tokyo, 2-11-16 Yayoi, Tokyo 113-8656, Japan

[4]Office of University Professors, The University of Tokyo, 2-11-16 Yayoi, Tokyo 113-8656, Japan

[5]Lead contact

*Correspondence: domen@chemsys.t.u-tokyo.ac.jp

https://doi.org/10.1016/j.joule.2023.05.018

Please cite this article in press as: Nandy et al., Oxide layer coating enabling oxysulfide-based photocatalyst sheet to drive Z-scheme water splitting at atmospheric pressure, Joule (2023), https://doi.org/10.1016/j.joule.2023.05.018

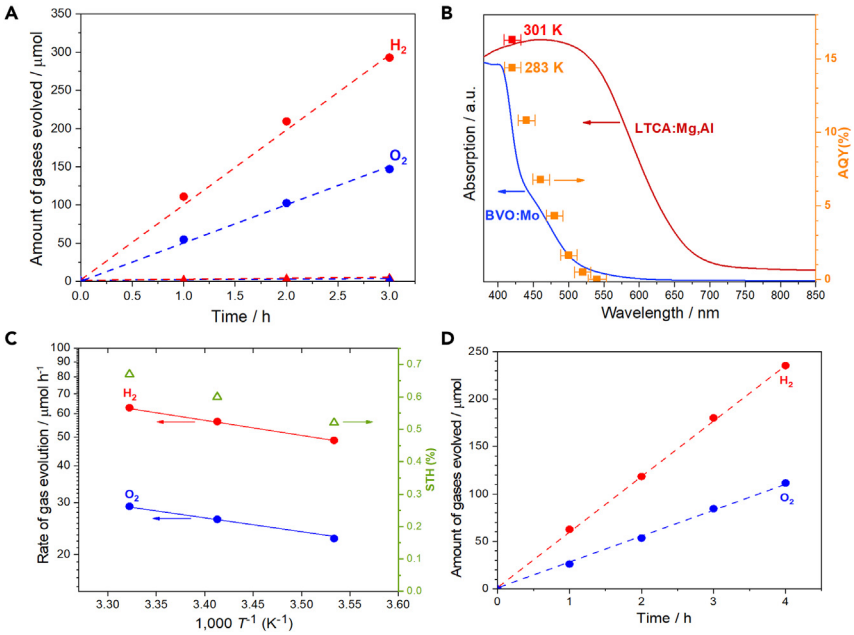

Figure 1. ZOWS activity of CoO_x/Cr_2O_3/Rh-loaded LTCA:Mg,Al/Au/BVO:Mo(h) sheets

(A) Time course of gas evolution during ZOWS at 2 kPa and 283 K with (circles) and without (triangles) the cocatalyst loading.

(B) AQY as a function of light wavelength at 283 K (orange squares) and at 301 K (red square), together with Kubelka-Munk functions for photocatalysts.

(C) Temperature (*T*) dependence of ZOWS activity and STH at initial background pressure of 2 kPa.

(D) Time course of gas evolution during ZOWS at 4 kPa and 301 K under simulated sunlight (AM 1.5G); irradiation area: 6.25 cm^2.

at around 690 nm irrespective of doping. LTCA:Mg,Al consisted of rod-like particles with average lengths of 5–8 μm, similar to the previously studied LTCA:Ga, as shown in the scanning electron microscopy (SEM) images in Figure S2C. BVO:Mo(h) and BVO:Mo(s-l) consisted of a well-crystallized monoclinic scheelite phase, as was confirmed from XRD patterns (Figure S3A).[10,24] A similar absorption onset was observed for both kinds of BVO:Mo (Figure S3B). BVO:Mo(h) and BVO:Mo(s-l) were composed of spherical particles 1 μm in size and plate-like particles 3 μm in size, respectively (Figure S3C).

Evaluation of ZOWS activity at reduced background pressure

Before the investigation of the reaction properties of the photocatalyst sheet for ZOWS under elevated pressure, screening of the HEP and OEP materials applied to the sheet was conducted. As shown in Table S1, after loading Cr_2O_3/Rh and CoO_x cocatalysts, LTCA/Au/BVO:Mo photocatalyst sheets using LTCA:Mg,Al as the HEP exhibited 35% higher ZOWS activity than those using LTCA:Ga under visible light irradiation at 2 kPa and 283 K, regardless of the type of BVO:Mo, although the structural features of the LTCA materials were similar. This is likely due to the improved controllability of cationic doping by applying the impregnation-calcination process before the synthesis of the LTCA phase. In addition, the photocatalyst sheets made from BVO:Mo(h) were 20% more active than those made from BVO:Mo(s-l), regardless of the dopants in LTCA, suggesting the benefit of using small BVO:Mo particles. Consequently, photocatalyst sheets consisting of LTCA:Mg,Al as the HEP and BVO:Mo(h) as the OEP achieved the highest activity (Figure 1A). The gas evolution rate of this photocatalyst sheet gradually decreased

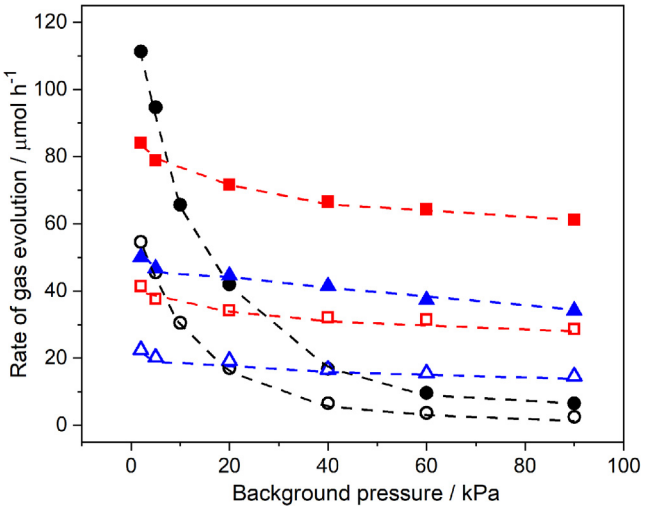

Figure 2. Background pressure dependence of ZOWS activity of LTCA:Mg,Al/Au/BVO:Mo(h) sheets

H_2 (closed symbols) and O_2 (open symbols) gas evolution rates for CoO_x/Cr_2O_3/Rh-loaded LTCA:Mg,Al/Au/BVO:Mo(h) sheets (9 cm^2) under visible light irradiation at 283 K and different background pressures before (circles) and after TiO_2 (triangles) or SiO_2 modification (squares)

as the reaction proceeded but was largely recovered after evacuation of the system, as shown in Figure S4, suggesting that the decrease of the gas evolution rates was due to backward reactions. Therefore, the sheet was regarded as stable for at least 20 h and was employed in subsequent experiments. Note that the bare photocatalyst sheet without cocatalysts loading evolved very small amounts of H_2 and O_2 under visible light (3.5 and 1.6 μmol in 3 h, respectively) due to the lack of surface-active sites for H_2 evolution. It is also noteworthy that the activity drastically decreased in the absence of Au conductor layer, indicating that the ZOWS reaction proceeded by charge transfer through the thin Au layer.[21]

Figure 1B presents action spectra of an LTCA:Mg,Al/Au/BVO:Mo(h) sheet modified with CoO_x/Cr_2O_3/Rh cocatalysts. The sample exhibited an AQY of 14.4% at 420 ± 10 nm in the ZOWS reaction at 283 K and 2 kPa. The AQY values decrease with increasing wavelengths of the incident light, and the sample utilizes visible light up to 520 nm, which is consistent with the absorption onset for BVO:Mo(h). Notably, upon increasing the temperature to 301 K at 4 kPa, the AQY at 420 ± 10 nm increases to 16.3%. Correspondingly, as shown in Figure 1C, the STH value measured under illumination by simulated sunlight increases from 0.52% at 2 kPa and 283 K to 0.67% at 4 kPa and 301 K. These AQY and STH values are among the highest ever reported for systems involving non-oxide particulate photocatalysts. Moreover, as shown in Figure 1D, the photocatalyst sheet maintains high ZOWS activity at 4 kPa and 301 K with intermittent cooling and evacuation of the reaction system for sampling.

The ZOWS activity for CoO_x/Cr_2O_3/Rh/LTCA:Mg,Al/Au/BVO:Mo(h) sheets was examined as a function of background pressure and temperature to monitor the influence of backward reactions on the photocatalytic performance of the sheets. As seen in Figure 2, the gas evolution rate decreases monotonically with increasing background Ar pressure at 283 K and drops by 90% by increasing the pressure from 2 to 90 kPa. This is considered to be due to backward reactions on the cocatalyst and the Au conductor layer. In a previous study on $SrTiO_3$:Rh,La-BVO:Mo

Please cite this article in press as: Nandy et al., Oxide layer coating enabling oxysulfide-based photocatalyst sheet to drive Z-scheme water splitting at atmospheric pressure, Joule (2023), https://doi.org/10.1016/j.joule.2023.05.018

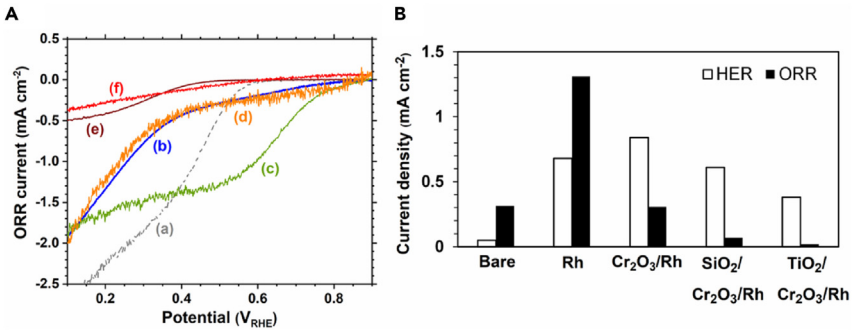

Figure 3. Photoelectrochemical properties of LTCA:Mg,Al/Au photoelectrodes

(A) Oxygen reduction current density for (a) bare Au/Ti, (b) unmodified LTCA:Mg,Al/Au, (c) Rh/LTCA:Mg,Al/Au, (d) Cr_2O_3/Rh/LTCA:Mg,Al/Au, (e) TiO_2/Cr_2O_3/Rh/LTCA:Mg,Al/Au, and (f) SiO_2/Cr_2O_3/Rh/LTCA:Mg,Al/Au photoelectrodes.

(B) Photocathodic HER and ORR current densities at +0.48 V vs. RHE for LTCA:Mg,Al/Au photocathodes after various surface modifications. Reaction conditions: 0.1 M Na_2SO_4 (pH 6.7) electrolyte solution saturated with O_2 (for ORR) or Ar (for HER) under visible light irradiation (λ > 420 nm) from a 300 W Xe lamp.

sheets, replacement of Au with C, which does not promote the ORR, mitigated this pressure dependence.[15] However, the activity of LTCA:Mg,Al-BVO:Mo sheets was still highly sensitive to the background pressure, even when a C conductor layer was used in our preliminary investigations. Therefore, the ORR on the LTCA:Mg,Al photocatalyst is likely a primary cause for the negative pressure dependence of ZOWS activity of the photocatalyst sheet.

Origin of backward reactions and effect of oxide layer coating onto ZOWS activity

To determine the impact of the ORR on the CoO_x/Cr_2O_3/Rh/LTCA:Mg,Al/Au/BVO:Mo(h) photocatalyst sheet, the (photo)electrochemical properties of LTCA:Mg,Al/Au with various surface modifications were studied. A Au layer deposited onto Ti foil was also examined as a reference. As seen in Figure 3, the Au/Ti electrode starts to generate an ORR current at +0.55 V vs. RHE, which is consistent with our earlier work.[15] The ORR onset potential for the LTCA:Mg,Al/Au photocathode under illumination is more positive (+0.85 V vs. RHE), indicating that photoexcited electrons in LTCA:Mg,Al certainly induced the ORR. The Rh/LTCA:Mg,Al/Au photocathode generates a higher current density because the Rh species catalyze the photoinduced ORR. Deposition of a Cr_2O_3 layer lowers the ORR current to a similar level to that for LTCA:Mg,Al/Au, suggesting that Cr_2O_3 forms a shell on the Rh cocatalyst and suppresses the ORR. However, Cr_2O_3 shell is not likely deposited sufficiently on the surface of LTCA:Mg,Al particles, and thus the ORR occurred persistently. Therefore, additional coating materials are necessary for the surface of LTCA:Mg,Al particles.

It is known that amorphous TiO_2 can be uniformly deposited by photodecomposition on photocatalyst particles using a titanium peroxide complex, and it can effectively suppress side reactions, including the ORR.[25] In fact, amorphous TiO_2 has been applied to Z-scheme photocatalyst sheets to mitigate backward reactions.[14] Therefore, the CoO_x/Cr_2O_3/Rh-modified LTCA:Mg,Al/Au/BVO:Mo(h) sheet was modified with an amorphous TiO_2 layer. The TiO_2-modified photocatalyst sheet exhibits the highest ZOWS activity at 90 kPa when the TiO_2 loading amount is 0.8 mg per 9 cm^2 (Figure S5). The resulting photocatalyst sheet maintains 70% ZOWS activity when the background pressure is increased from 2 to 90 kPa (Figure 2). In

Please cite this article in press as: Nandy et al., Oxide layer coating enabling oxysulfide-based photocatalyst sheet to drive Z-scheme water splitting at atmospheric pressure, Joule (2023), https://doi.org/10.1016/j.joule.2023.05.018

accordance with this, deposition of amorphous TiO_2 in addition to Cr_2O_3 onto the Rh/LTCA:Mg,Al/Au photocathode suppressed the ORR current more effectively, shifting the onset potential to +0.45 V vs. RHE (Figure 3A). However, the ZOWS activity at 2 kPa decreased by 50% compared with the original activity before TiO_2 coating, and the TiO_2-coated photocatalyst sheet achieved an STH of 0.19% at 301 K. In fact, the photocathodic hydrogen evolution reaction (HER) current for the Cr_2O_3/Rh/LTCA:Mg,Al photocathode at 0.48 V vs. RHE, in which the CoO_x/Cr_2O_3/Rh-modified LTCA:Mg,Al/Au/BVO:Mo(h) sheet was considered to operate during the ZOWS reaction (Figure S6), was reduced by 2.2 times by depositing amorphous TiO_2 (Figures 3B and S7). Using a lower amount of TiO_2 preserved the ZOWS activity at reduced pressure better, but the pressure dependence became larger. Moreover, the TiO_2-modified photocatalyst sheet lost almost all ZOWS activity when the reaction temperature was raised to 318 K, and the activity was not recovered even after cooling to 283 K (Figure S8). The HER current was also decreased when a TiO_2-coated Cr_2O_3/Rh/LTCA:Mg,Al/Au photocathode underwent a heat treatment at 318 K (Figure S9). This is because amorphous TiO_2 was condensed, and the permeability to reactants (H^+ and H_2O) was reduced irreversibly, as was reported for OWS systems based on TiO_2/$RhCrO_y$/$LaMg_{1/3}Ta_{2/3}O_2N$ and TiO_2/Al-doped $SrTiO_3$.[26,27] The temperature of the water reactant is expected to exceed 313 K under realistic outdoor operating conditions for solar energy harvesting systems,[5] TiO_2 is not a practical option for mitigating the pressure dependence of ZOWS activity.

Based on a survey of hydrothermally stable amorphous oxide materials, amorphous SiO_2 hydrolyzed from tetraethylorthosilicate (TEOS) was found to be durable in hot water and suppress the ORR while preserving the HER activity. The ZOWS activity as a function of the background Ar pressure for CoO_x/Cr_2O_3/Rh/LTCA:Mg,Al/Au/BVO:Mo(h) modified with SiO_2 is presented in Figure 2. The activity is reduced by 27% by raising the pressure from 2 to 90 kPa, but this reduction is less than that without any surface modification or with TiO_2 modification. As seen in Figure S10, the optimum amount of SiO_2 is 8.1 mg per 9 cm^2 in which the SiO_2-modified photocatalyst sheet exhibits the highest ZOWS activity at 90 kPa. Under near-atmospheric pressure, the sheet stably evolved H_2 and O_2 gases in a stoichiometric ratio of 2:1 for several hours (Figure 4A). The ZOWS activity was also investigated at temperatures ranging from 283 to 333 K at 90 kPa under simulated sunlight (Figure 4B). The ZOWS activity increases with increasing temperature, reaching an AQY of 9.7% at 333 K at a wavelength of 420 nm, with an STH value of 0.41%. The apparent activation energy was estimated to be 14 kJ mol^{-1} from the Arrhenius plot, which is comparable to the value observed for LTCA:Ga/Au/BVO(s-l) sheets.[10] Moreover, the photocatalyst sheet decomposed water stably for at least 4 h under these conditions with intermittent cooling and evacuation of the reaction system (Figure 4C). A scanning transmission electron microscopy-energy dispersive X-ray spectroscopy (STEM-EDS) analysis of the photocatalyst sheet sample subjected to the ZOWS reaction revealed the formation of an amorphous SiO_2 layer about 5–8 nm in thickness on both LTCA:Mg,Al and BVO(h) (Figure 5). The results of an X-ray photoelectron spectroscopy (XPS) analysis also indicated coating of both LTCA:Mg,Al and BVO(h) with SiO_2, because the signals from the elements in the photocatalysts became weaker and a Si 2*p* peak indicative of the presence of SiO_2 appeared (Figure S11). However, prominent peaks associated with LTCA:Mg,Al, BVO(h), and Au (e.g., Cu 2*p*, Bi 4*f*, and Au 4*f* peaks, respectively) were still observed. Therefore, the photocatalyst sheet was not uniformly coated with SiO_2, which explains the mild pressure dependence of the ZOWS activity after modification of the photocatalyst sheet with SiO_2.

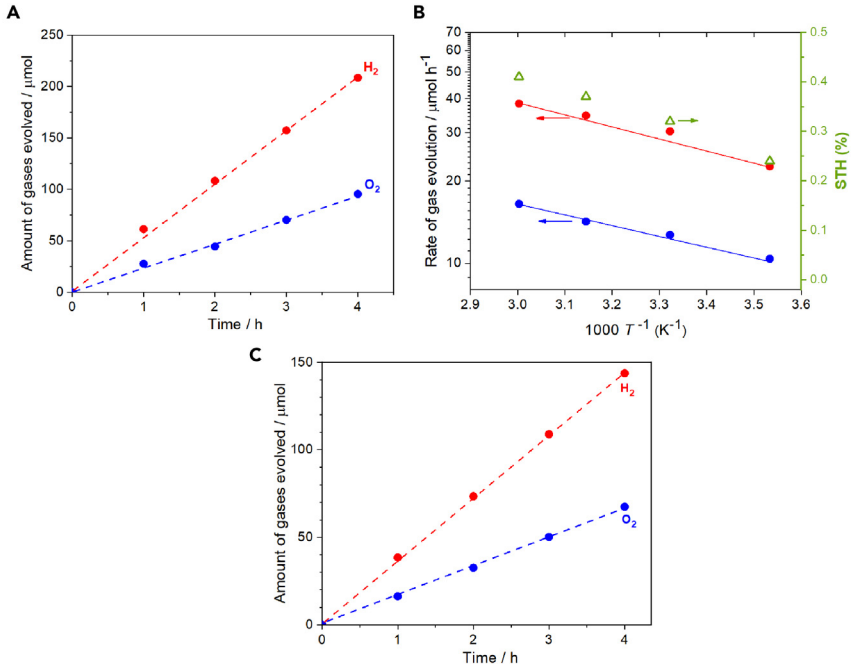

Figure 4. ZOWS Activity of SiO_2-coated LTCA:Mg,Al/Au/BVO:Mo(h) sheets at elevated pressure

(A) Time course of gas evolution during ZOWS reaction using SiO_2-coated CoO_x/Cr_2O_3/Rh-coloaded LTCA:Mg,Al/Au/BVO:Mo(h) photocatalyst sheet (9 cm^2) at initial background pressure of 90 kPa and temperature of 283 K under visible light (λ > 420 nm) irradiation from 300 W Xe lamp. (B and C) (B) Temperature dependence (*T*) of ZOWS activity and STH for SiO_2-modified photocatalyst sheets and (C) time course of gas evolution during the ZOWS at 333 K at 90 kPa under simulated sunlight (AM1.5G, 6.25 cm^2).

The ZOWS activity of CoO_x/Cr_2O_3/Rh-loaded LTCA:Mg,Al/Au/BVO:Mo(h) sheets modified with SiO_2 and TiO_2 layers under simulated sunlight at 90 kPa as a function of temperature is summarized in Table S2. The TiO_2 layer condensed and degraded the ZOWS activity of the sheet irreversibly at a temperature higher than 303 K. However, this problem was overcome by using SiO_2 layer coating, which was durable under hot water and elevated pressure.

Our group reported that SiO_2 coating could improve the water splitting activity of $TiO_2/RhCrO_x/LaMg_{1/3}Ta_{2/3}O_2N$ by adjusting the density and permeability of the coating layer. However, the reaction was investigated only under low pressure and temperature, and the benefit of SiO_2 on the suppression of backward reaction and pressure dependence of the water splitting activity was undiscovered. In the present work, the SiO_2 coating was considered to suppress the ORR occurring on the LTCA:Mg,Al surface while preserving the HEP and OEP activity. To verify the functionality of SiO_2, the Au/Ti electrode, Cr_2O_3/Rh/LTCA:Mg,Al/Au photocathode, and BVO:Mo(h)/Au photoanode were modified with SiO_2 in the same manner and subjected to photoelectrochemical measurements. Amorphous silica layer suppressed the extent of ORR occurring on the Au layer (Figure S12). The SiO_2/Cr_2O_3/Rh/LTCA:Mg,Al/Au photocathode generated an ORR current of 0.05 mA cm^{-2} at 0.48 V vs. RHE under irradiation (Figure 3). This is 77% lower than that for the Cr_2O_3/Rh/LTCA:Mg,Al/Au photoelectrode, but is still less effective than modification with amorphous TiO_2. However, the SiO_2 modification preserved 70% of the HER activity of the Cr_2O_3/Rh/LTCA:Mg,Al/Au photoelectrode, whereas the TiO_2 modification preserved only 45%. Moreover, SiO_2 deposition effectively suppressed

Please cite this article in press as: Nandy et al., Oxide layer coating enabling oxysulfide-based photocatalyst sheet to drive Z-scheme water splitting at atmospheric pressure, Joule (2023), https://doi.org/10.1016/j.joule.2023.05.018

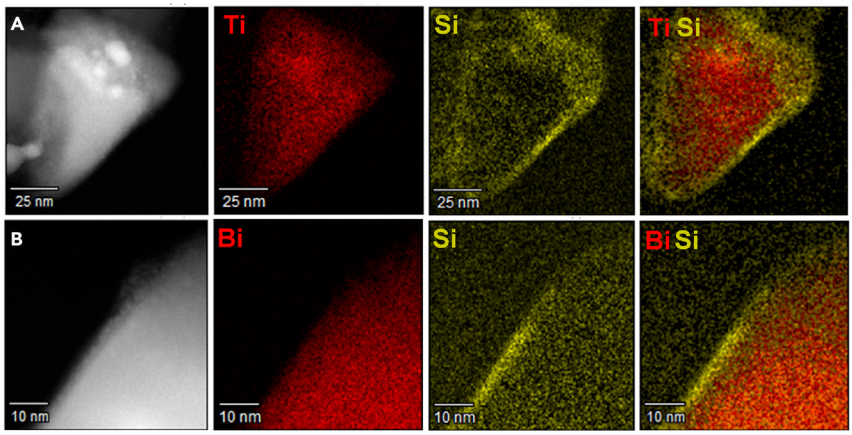

Figure 5. ADF-STEM image and STEM-EDS elemental maps of SiO_2-coated photocatalyst sheets
Cross-sectional sample of (A) LTCA:Mg,Al and (B) BVO:Mo(h) particles obtained from LTCA:Mg,Al/Au/BVO:Mo(h) photocatalyst sheet loaded with cocatalysts, modified with amorphous SiO_2, and subjected to ZOWS reaction.

the ORR even after a heat treatment at 333 K in water (Figure S13). In addition, the SiO_2 coating had no negative effect on the oxygen evolution activity of BVO:Mo(h) judging from the similar photoanodic currents observed for BVO:Mo(h)/Au photoanodes before and after the SiO_2 coating (Figure S14). Owing to the balance between suppressing the ORR and maintaining the HER and OER activity, in addition to thermal stability, it can be concluded that the SiO_2-modified photocatalyst sheet exhibits excellent ZOWS activity at elevated pressure and temperature. Nevertheless, the SiO_2 coating did lower the ZOWS activity. At a low pressure of 4 kPa and a temperature of 301 K, the STH value of the cocatalyst-loaded LTCA:Mg,Al/Au/BVO:Mo(h) photocatalyst sheet was decreased from 0.67% to 0.52% upon the SiO_2 coating, probably due to partial blockage of the H_2 evolution sites at thicker parts of the coating as a result of the inhomogeneous coating. Moreover, the long-term durability of the SiO_2-modified photocatalyst sheet under elevated pressure and temperature is yet to be investigated. These aspects need to be addressed in follow-up studies.

In conclusion, the LTCA:Mg,Al/Au/BVO:Mo(h) particulate photocatalyst sheet loaded with Cr_2O_3/Rh and CoO_x cocatalysts split water into H_2 and O_2 with an AQY and STH of 16.3% (at 420 nm) and 0.67% (under AM 1.5G), respectively, at 4 kPa and 301 K. However, the ZOWS activity for the sheet decreased sharply with increasing background pressure because of the ORR occurring on Cr_2O_3/Rh/LTCA:Mg,Al serving as the HEP. The Cr_2O_3 coating suppressed the ORR on the Rh cocatalyst but not sufficiently on the exposed LTCA:Mg,Al photocatalyst. An amorphous SiO_2 layer deposited by hydrolysis of TEOS was found to cover the surface of the photocatalyst sheet to a thickness of 5–8 nm and suppressed the ORR while largely preserving the activities of the LTCA:Mg,Al and BVO:Mo(h). Moreover, the SiO_2 layer was durable in hot water. As a result, the cocatalyst-loaded LTCA:Mg,Al/Au/BVO:Mo(h) sheet modified with amorphous SiO_2 layer exhibited an STH of 0.41% at 90 kPa and 333 K, which approximated practical operating conditions. This work demonstrates the activation of photocatalyst sheets involving a narrow band-gap oxysulfide HEP prone to the ORR under typical outdoor operating conditions and will contribute to the development of highly efficient ZOWS systems for realizing large-scale solar fuel production.

Please cite this article in press as: Nandy et al., Oxide layer coating enabling oxysulfide-based photocatalyst sheet to drive Z-scheme water splitting at atmospheric pressure, Joule (2023), https://doi.org/10.1016/j.joule.2023.05.018

EXPERIMENTAL PROCEDURES

Resource availability

Lead contact

Further information and requests for resources should be directed to the lead contact, Kazunari Domen (domen@chemsys.t.u-tokyo.ac.jp).

Materials availability

Materials generated in this study will be made available on request, but we may require a payment and/or a completed materials transfer agreement if there is potential for commercial application.

Data and code availability

All data will be made available upon reasonable request.

Preparation of photocatalysts

Doped LTCA was synthesized by a solid-state reaction (SSR).[10] To control the dopant concentration at the level of 1 mol % (with respect to Ti) Mg^{2+} (Mg/Ti + Mg + Al = 1 mol %) and Al^{3+} (Al/Ti + Mg + Al = 1 mol %) were co-doped into TiO_2 by impregnation and calcination (1,073 K for 1 h) before mixing with other precursor chemicals. After that, TiO_2:Mg,Al, La_2O_3, La_2S_3, Cu_2S, Ag_2S, and S were blended in a molar ratio of 8:12:16:3.6:0.4:1 in a nitrogen filled glovebox, sealed in evacuated quartz tubes, and heated at 1,323 K for 96 h. The solid chunk obtained was ground into powder. Ga-doped LTCA was also synthesized, where TiO_2 was replaced with Ga_2O_3 so that the Ti:Ga molar ratio became 99:1. BVO:Mo samples were prepared by a solid-liquid reaction and a hydrothermal reaction following the literature and are denoted as BVO:Mo(s-l) and BVO:Mo(h), respectively.[10,24]

Preparation of photocatalyst sheets

Photocatalyst sheets were fabricated by a particle transfer method using Au as a conductor material (Figure S1).[10,14,15] Doped-LTCA/Au/BVO:Mo photocatalyst sheets were loaded with Cr_2O_3/Rh and CoO_x cocatalysts following our previous study.[21] Subsequently, the photocatalyst sheets were coated with amorphous SiO_2 or TiO_2 by hydrolysis or photodecomposition, respectively.[26]

Photocatalytic water splitting reaction

The ZOWS activity of the modified LTCA:Mg,Al/Au/BVO:Mo sheets was measured using a closed gas-circulation system. A representative structure of the system has been reported elsewhere.[28] A photocatalyst sheet sample with an effective area of ~9 cm^2 was placed at the bottom of a top-irradiation type reactor made of Pyrex glass, and 40 mL of distilled water without pH adjustment was added to the reactor. The reactor was evacuated thoroughly to remove air. Unless otherwise noted, the reaction was carried out at an initial pressure of 2 kPa and a temperature of 283 K. In some experiments, the initial background pressure and temperature were controlled in the ranges of 2–90 kPa and 283–333 K by introducing Ar into the reaction system and warming the solution using a water bath, respectively. The evolved gas amounts were analyzed by a gas chromatograph equipped with a thermal conductivity detector and a molecular sieve with 5 Å columns that was directly connected to the closed gas-circulation system. One notable structural feature of the closed gas-circulation system is that it has condensers between the illuminated reactor at the bottom and the gas sampler to extract the product gas at the top. When the reaction solution boils at a low pressure and elevated temperature, water vapor condenses at the condensers, enriching the upper part of the system where the gas sampler is installed with hydrogen and oxygen and the lower part with water vapor. This results in

overestimation of the gas amount in the system. To ensure the homogeneity of the gas components in the closed system, the reaction solution was sufficiently cooled for each sample when the temperature was intentionally raised.

SUPPLEMENTAL INFORMATION

Supplemental information can be found online at https://doi.org/10.1016/j.joule.2023.05.018.

ACKNOWLEDGMENTS

This research work was financially supported by the Artificial Photosynthesis Project (ARPChem) of the New Energy and Industrial Technology Development Organization (NEDO) and by JST, PRESTO, Japan (grant no. JPMJPR20T9). Part of this study was supported by the University of Tokyo Advanced Characterization Nanotechnology Platform as part of the Nanotechnology Platform Project sponsored by the Ministry of Education, Culture, Sports, Science, and Technology (MEXT), Japan (grant no. JPMXP09A-22-UT-0023). The authors thank Mr. Atsushi Ohnishi from the University of Tokyo for carbon deposition and Ms. Michiko Obata from Shinshu University for her assistance in XPS analyses.

AUTHOR CONTRIBUTIONS

K.D. led the research project. S.N. surveyed the sample preparation, evaluated the photocatalytic activity, and verified the AQY and STH values. M.N. and N.S. carried out the STEM measurements. H.L. assisted in the hydrothermal synthesis of BVO. S.N., T.H., M.N., X.W., H.L., N.S., T.T., and K.D. discussed the results. T.H. and K.D. supervised the research work. S.N., T.H., and K.D. wrote the manuscript and revised it with contributions from the other authors.

DECLARATION OF INTERESTS

K.D. is an advisory board member of this journal.

INCLUSION AND DIVERSITY

We support inclusive, diverse, and equitable conduct of research.

Received: February 2, 2023
Revised: April 24, 2023
Accepted: May 22, 2023
Published: June 14, 2023

REFERENCES

1. Hisatomi, T., and Domen, K. (2019). Reaction systems for solar hydrogen production via water splitting with particulate semiconductor photocatalysts. Nat. Catal. *2*, 387–399.

2. Wang, Y., Suzuki, H., Xie, J., Tomita, O., Martin, D.J., Higashi, M., Kong, D., Abe, R., and Tang, J. (2018). Mimicking natural photosynthesis: solar to renewable H2 fuel synthesis by Z-scheme water splitting systems. Chem. Rev. *118*, 5201–5241.

3. Nandy, S., Savant, S.A., and Haussener, S. (2021). Prospects and challenges in designing photocatalytic particle suspension reactors for solar fuel processing. Chem. Sci. *12*, 9866–9884.

4. Takata, T., Jiang, J., Sakata, Y., Nakabayashi, M., Shibata, N., Nandal, V., Seki, K., Hisatomi, T., and Domen, K. (2020). Photocatalytic water splitting with a quantum efficiency of almost unity. Nature *581*, 411–414.

5. Nishiyama, H., Yamada, T., Nakabayashi, M., Maehara, Y., Yamaguchi, M., Kuromiya, Y., Nagatsuma, Y., Tokudome, H., Akiyama, S., Watanabe, T., et al. (2021). Photocatalytic solar hydrogen production from water on a 100-m^2 scale. Nature *598*, 304–307.

6. Wang, Q., Nakabayashi, M., Hisatomi, T., Sun, S., Akiyama, S., Wang, Z., Pan, Z., Xiao, X., Watanabe, T., Yamada, T., et al. (2019). Oxysulfide photocatalyst for visible- light-driven overall water splitting. Nat. Mater. *18*, 827–832.

7. Tao, X., Zhao, Y., Wang, S., Li, C., and Li, R. (2022). Recent advances and perspectives for solar- driven water splitting using particulate photocatalysts. Chem. Soc. Rev. *51*, 3561–3608.

8. Maeda, K. (2013). Z-scheme water splitting using two different semiconductor photocatalysts. ACS Catal. *3*, 1486–1503.

9. Segev, G., Kibsgaard, J., Hahn, C., Xu, Z.J., Cheng, W.-H., Deutsch, T.G., Xiang, C., Zhang, J.Z., Hammarström, L., Nocera, D.G., et al. (2022). The 2022 solar fuels roadmap. J. Phys. D *55*, 323003.

10. Sun, S., Hisatomi, T., Wang, Q., Chen, S., Ma, G., Liu, J., Nandy, S., Minegishi, T., Katayama, M., and Domen, K. (2018). Efficient redox-mediator-free Z-scheme water splitting employing oxysulfide photocatalysts under visible light. ACS Catal. *8*, 1690–1696.

11. Iwase, A., Ng, Y.H., Ishiguro, Y., Kudo, A., and Amal, R. (2011). Reduced graphene oxide as a solid-state electron mediator in Z-scheme photocatalytic water splitting under visible light. J. Am. Chem. Soc. *133*, 11054–11057.

12. Ogawa, K., Suzuki, H., Zhong, C., Sakamoto, R., Tomita, O., Saeki, A., Kageyama, H., and Abe, R. (2021). Layered perovskite oxyiodide with narrow band gap and long lifetime carriers for water splitting photocatalysis. J. Am. Chem. Soc. *143*, 8446–8453.

13. Yoshino, S., Iwase, A., Ng, Y.H., Amal, R., and Kudo, A. (2020). Z-schematic solar water splitting using fine particles of H2-evolving (CuGa)0.5ZnS2 photocatalyst prepared by a flux method with chloride salts. ACS Appl. Ener. Mater. *3*, 5684–5692.

14. Wang, Q., Hisatomi, T., Jia, Q., Tokudome, H., Zhong, M., Wang, C., Pan, Z., Takata, T., Nakabayashi, M., Shibata, N., et al. (2016). Scalable water splitting on particulate photocatalyst sheets with a solar-to-hydrogen energy conversion efficiency exceeding 1%. Nat. Mater. *15*, 611–615.

15. Wang, Q., Hisatomi, T., Suzuki, Y., Pan, Z., Seo, J., Katayama, M., Minegishi, T., Nishiyama, H., Takata, T., Seki, K., et al. (2017). Particulate photocatalyst sheets based on carbon conductor layer for efficient Z-scheme pure-water splitting at ambient pressure. J. Am. Chem. Soc. *139*, 1675–1683.

16. Wang, Q., Okunaka, S., Tokudome, H., Hisatomi, T., Nakabayashi, M., Shibata, N., Yamada, T., and Domen, K. (2018). Printable photocatalyst sheets incorporating a transparent conductive mediator for Z-scheme water splitting. Joule *2*, 2667–2680.

17. Pan, Z., Hisatomi, T., Wang, Q., Chen, S., Nakabayashi, M., Shibata, N., Pan, C., Takata, T., Katayama, M., Minegishi, T., et al. (2016). Photocatalyst sheets composed of particulate $LaMg_{1/3}Ta_{2/3}O_2N$ and Mo-doped $BiVO_4$ for Z-scheme water splitting under visible light. ACS Catal. *6*, 7188–7196.

18. Hisatomi, T., Okamura, S., Liu, J., Shinohara, Y., Ueda, K., Higashi, T., Katayama, M., Minegishi, T., and Domen, K. (2015). La5Ti2Cu1-xAgxS5O7 photocathodes operating at positive potentials during photoelectrochemical hydrogen evolution under irradiation of up to 710 nm. Energy Environ. Sci. *8*, 3354–3362.

19. Meignen, V., Cario, L., Lafond, A., Moëlo, Y., Guillot-Deudon, C., and Meerschaut, A. (2004). Crystal structures of two new oxysulfides La5Ti2*M*S5O7 (*M*=Cu, Ag): evidence of anionic segregation. J. Solid State Chem. *177*, 2810–2817.

20. Liu, J., Hisatomi, T., Ma, G., Iwanaga, A., Minegishi, T., Moriya, Y., Katayama, M., Kubota, J., and Domen, K. (2014). Improving the photoelectrochemical activity of La5Ti2CuS5O7 for hydrogen evolution by particle transfer and doping. Energy Environ. Sci. *7*, 2239–2242.

21. Chen, S., Nandy, S., Vequizo, J.J.M., Hisatomi, T., Nakabayashi, M., Pan, Z., Xiao, Q., Wang, Z., Lin, L., Sun, S., et al. (2023). Promotion of charge carriers utilization over $La_5Ti_2Cu_{0.9}Ag_{0.1}O_7S_5$-based photocatalyst sheet for efficient Z-scheme overall water splitting. ACS Catal. *13*, 3285–3294.

22. Zhao, D., Wang, Y., Dong, C.L., Huang, Y.C., Chen, J., Xue, F., Shen, S., and Guo, L. (2021). Boron-doped nitrogen-deficient carbon nitride-based Z-scheme heterostructures for photocatalytic overall water splitting. Nat. Energy *6*, 388–397.

23. Cao, Y., Liu, Y., Zakeeruddin, S.M., Hagfeldt, A., and Grätzel, M. (2018). Direct contact of selective charge extraction layers enables high-efficiency molecular photovoltaics. Joule *2*, 1108–1117.

24. Qi, Y., Zhao, Y., Gao, Y., Li, D., Li, Z., Zhang, F., and Li, C. (2018). Redox-based visible-light-driven Z- scheme overall water splitting with apparent quantum efficiency exceeding 10%. Joule *2*, 2393–2402.

25. Takata, T., Pan, C., Nakabayashi, M., Shibata, N., and Domen, K. (2015). Fabrication of a core−shell-type photocatalyst via photodeposition of Group IV and V transition metal oxyhydroxides: an effective surface modification method for overall water splitting. J. Am. Chem. Soc. *137*, 9627–9634.

26. Pan, C., Takata, T., Nakabayashi, M., Matsumoto, T., Shibata, N., Ikuhara, Y., and Domen, K. (2015). A complex perovskite-type oxynitride: the first photocatalyst for water splitting operable at up to 600 nm. Angew. Chem. Int. Ed. *127*, 2998–3002.

27. Suguro, T., Kishimoto, F., Kariya, N., Fukui, T., Nakabayashi, M., Shibata, N., Takata, T., Domen, K., and Takanabe, K. (2022). A hygroscopic nano-membrane coating achieves efficient vapor-fed photocatalytic water splitting. Nat. Commun. *13*, 5698.

28. Qureshi, M., and Takanabe, K. (2017). Insights on measuring and reporting heterogeneous photocatalysis: efficiency definitions and setup examples. Chem. Mater. *29*, 158–167.